RI | 9279

REPORT OF INVESTIGATIONS/1989

Yielding Steel Posts

By J. P. Dunford and L. N. Henton

BUREAU OF MINES

UNITED STATES DEPARTMENT OF THE INTERIOR

Mission: As the Nation's principal conservation agency, the Department of the Interior has responsibility for most of our nationally-owned public lands and natural and cultural resources. This includes fostering wise use of our land and water resources, protecting our fish and wildlife, preserving the environmental and cultural values of our national parks and historical places, and providing for the enjoyment of life through outdoor recreation. The Department assesses our energy and mineral resources and works to assure that their development is in the best interests of all our people. The Department also promotes the goals of the Take Pride in America campaign by encouraging stewardship and citizen responsibility for the public lands and promoting citizen participation in their care. The Department also has a major responsibility for American Indian reservation communities and for people who live in Island Territories under U.S. Administration.

Report of Investigations 9279

Yielding Steel Posts

By J. P. Dunford and L. N. Henton

UNITED STATES DEPARTMENT OF THE INTERIOR
Manuel Lujan, Jr., Secretary

BUREAU OF MINES
T S Ary, Director

Library of Congress Cataloging in Publication Data:

Dunford, J. P. (John P.)
Yielding steel posts / by J. P. Dunford and L. N. Henton

(Report of investigations / United States Department of the Interior, Bureau of Mines)

Includes bibliographical references.

Supt. of Docs. no.: I 2823:9279.

1. Ground control (Mining). 2. Columns, Iron and steel. I. Henton, L. N. (Laurin N.). II. Title. III. Series: Report of investigations (United States. Bureau of Mines); 9279.

TN23.U43 [TN288] 622 s–dc20 [622'.28] 89-600164

CONTENTS

ILLUSTRATIONS

UNIT OF MEASURE ABBREVIATIONS USED IN THIS REPORT

ft	foot	lbf	pound (force)
in	inch	min	minute
lb	pound (mass)		

YIELDING STEEL POSTS

By J. P. Dunford[1] and L. N. Henton[1]

ABSTRACT

This U.S. Bureau of Mines report describes the development of a yielding steel post for underground mine support. The report covers concept development, laboratory tests, modifications, and field evaluations.

The objective of this work was to develop a stiff support member capable both of supporting high loads and yielding when excessive amounts of mine entry closure were present. The 6- to 7-ft steel post was designed to yield nearly 2 ft while maintaining a 45-ton (force) load. The post is a three-piece unit consisting of top and bottom telescoping legs and a separate foot bracket. It develops its load-carrying characteristics when the lower pipe, with an attached interference ring, is forced into the larger top pipe.

Laboratory tests were used to determine critical loads and post performance for various post lengths. Field tests showed that the posts could perform in actual mining conditions. The post has the ability to provide support in highly yielding ground and also, because of its slender profile, enhance ventilation and provide more area for travelways and escapeways. The design is simple enough to allow for fabrication at most mine shop facilities.

[1]Mining engineer, Spokane Research Center, U. S. Bureau of Mines, Spokane, WA.

INTRODUCTION

A problem in underground mining is stabilization of excavations in highly yielding rock masses. After an excavation is made, the surrounding strata may be displaced into the entry, causing rib slough, roof sag, and floor heave. This displacement reduces the area available for ventilation, travelways, and escapeways.

Entries used in retreat longwall mining typically are subjected to three different stages of loading: when the entry is initially developed for use as a headgate, when the longwall face retreats along the entry during its use as a headgate, and when the adjacent longwall panel is mined and the entry is used as the tailgate. The tailgate must then be maintained after mining is completed for ventilation and as an escapeway.

Currently, most artificial roof supports in coal mines consist of roof bolts, wooden posts and cribs, and concrete cribs. Wood supports are readily available, easy to handle, and are inexpensive compared to steel and concrete supports. Wood has some disadvantages, however.

1. Although wood is very strong when loaded parallel to the grain, its strain capacity is limited; conversely, when loaded perpendicular to the grain, wood has a better strain capacity but it is much weaker.
2. The strength of wood can vary significantly with each individual piece, with the result being that a structure made from wood, such as a crib, is only as strong as its weakest part.
3. The bulkiness of wooden cribs and posts reduces the amount of air flow.
4. Wood is a flammable material and can promote mine fires.
5. Wood is susceptible to decay.

Many underground support problems could be eliminated if a simple substitute support could be designed. Such a support would need to have a load capacity equal to or greater than wood, a consistent yield mechanism, and a substantial yield length. It should be easy to install and relatively inexpensive.

This report summarizes recent research and development by the U.S. Bureau of Mines to produce such a post. Several design approaches were pursued, two of which are reported here: (1) splitting the barrels of two tubes and forcing them over one another while using pipe clamps for additional friction force, and (2) on the basis of tube expansion theory, forcing an oversized ring into the inside diameter (ID) of a thick-walled pipe, causing it to yield radially. After extensive laboratory testing and several modifications to the original designs, a functional, three-piece yielding steel post (figs. 1-2) was developed and produced by the Bureau.

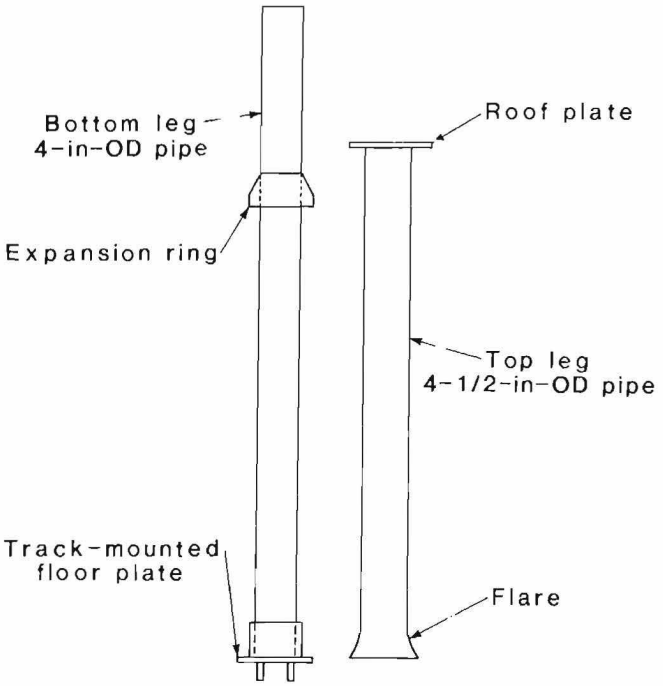

Figure 1.–Yielding steel post.

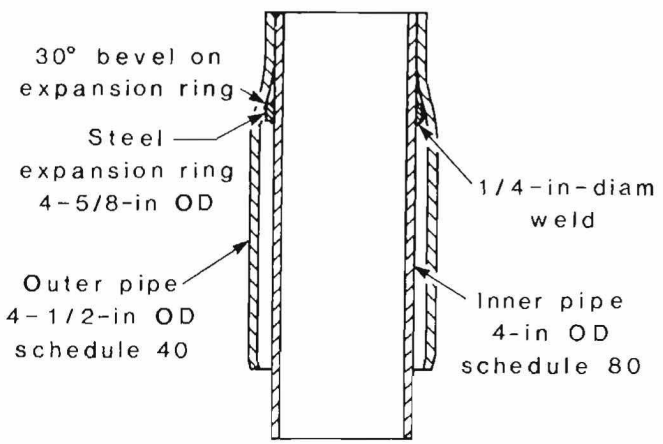

Figure 2.–Radial deformation of yielding steel post.

APPROACH

Before a preliminary design could be made, it was necessary to determine the requirements for a support that could be used in highly yielding ground. After such design requirements were established, prototypes were built and tested in the laboratory. Modifications were made on the basis of the test results until a working prototype was developed.

The design was based on a combination of performance, ease of fabricating and handling, and economic considerations. Performance of the wood and steel supports currently used for column-type supports were analyzed. Factors such as typical mine roof and floor compressive strengths and displacements, average longwall mining heights for Western coal mines, and overburden thicknesses were taken into account.

Ease of handling was also an important design consideration. The weight of the supports was restricted to what could normally be lifted by one individual. Special installation equipment was to be avoided because of added cost and the lack of working space in an entry.

Cost of the new support system was an important criterion. Wood and concrete crib support systems were compared with yielding steel posts in terms of material cost, fabrication cost, and shipment to and installation in the mine. The assumptions and calculations used to make these comparisons are given in appendix A.

A market survey was conducted to determine if similar supports were already being manufactured, especially supports with high-capacity and high-yield features. It was found that one manufacturer does produce a support using a design similar to the yielding arch concept. This type of support develops load resistance from the sliding friction between clamped legs. A number of supports were tested but they did not meet design specifications; that is, they lacked the load capacity and yield characteristics desired.

After the design requirements were established, appropriate materials were selected and the yield mechanism was developed. Wood, steel, concrete, and composite materials were evaluated, and steel was chosen because of its availability, high strength, nonflammability, and relatively low cost.

Design requirements for the new support were as follows:

1. The mechanism must have at least a 50-ton[2] capacity, based upon the average strength of a 6- to 8-in-diameter wood post.
2. It must maintain a controlled closure up to 6 in, which is acceptable in a coal seam greater than 60 in.
3. It should be as slender as possible, to prevent interference with ventilation.
4. It should be easy to manufacture, ideally in a mine shop.
5. Operation should be simple, reducing the risk of poor installation.
6. It should be easy to install, reducing injuries and cost.
7. It should cost less than $200 to manufacture.

[2]In this report, "tons" refers to tons of force (2,000 lbf).

POST DESIGN

The first designs tested utilized the clamp-and-sliding-friction concept for developing load characteristics. It was found that loading was a function of both the number of bolts used and the torque applied to the bolts. To obtain the 50-ton design limit, more than ten 3/4-in bolts (five clamps) were used without much success.

At this point a decision was made to utilize the physical properties and geometry of steel pipe. In the first attempt, a series of slots was cut into a pipe. This pipe was then forced into a second, slightly larger pipe, causing friction and deformation of the first (slotted) pipe, which in turn created load resistance. Results were inconsistent and the design did not allow for large amounts of yield. However, deformation of the outer pipe observed during testing led to the concept of producing load resistance by deliberately causing the outer pipe to yield.

To develop the loads required to deform a steel pipe, a weld bead was applied around the outside circumference of the smaller pipe. The increase in diameter on the inner pipe caused interference when the pipes were forced together. This worked better and had much more potential for yield, but again, the load capacity at the yield point was inconsistent.

The most successful design tested consisted of an expansion (interference) ring welded to the outside surface of the smaller pipe. The two pipes were then forced together until the ring caused the larger pipe to deform radially (fig. 2). This behavior is similar to that occurring in the extrusion process for manufacturing seamless pipe.

LABORATORY EVALUATION

When initial testing and theory indicated that the interference mechanism would generate a controlled, predictable yield in the laboratory, additional performance characteristics representing the loads, loading patterns, and support height requirements of actual mining conditions needed to be developed. Using the initial design criteria and information obtained from several Western mines concerning gate road entries and ground response during longwall mining, the following support requirements were set:

1. The upper height limit for the support prototype would be 84 in.
2. The weight would not exceed 120 lb for the total support.

3. The support should have a capacity of 45 to 50 tons.[3]

4. The support should be capable of yielding up to 24 in.

Initial testing indicated that to obtain the required load capacity and yield characteristics prior to buckling, the pipe column must be 3 to 4 in. in diameter and have walls between 1/4 and 1/2 in thick. In addition, to develop a 40- to 50-ton capacity, an interference of at least 1/2 in is required. For economic and availability reasons, 4-in, ASTM-120, schedule 40 seamed pipe was selected for the top (yielding) leg and 3-1/2-in, ASTM A-120, schedule 80 pipe was used for the bottom (force) leg. The expansion ring material was cut from 4-3/4-in cylindrical tube stock. This created a tight fit with the 3-1/2-in pipe and produced better alignment during the welding process.

The prototype design consisted of a top leg with a flared end and a bottom leg with an expansion ring that had been lathed to a predetermined outside diameter (OD). To determine what OD was required, early testing indicated that dimensions of the top leg ID were critical. The ID of ASTM A-120 pipe does not have to conform to strict specifications; discrepancies in excess of 0.010 in are common and some as large as 0.075 in have been measured. Therefore it was critical to the performance of the unit to first measure the pipe ID and then lathe the expansion ring to a specific OD so that the predetermined interference was correct.

[3]Bowers, E. T., and L. N. Henton. A Summary of Data From the Sunnyside Single Entry Study–1971-80. BuMines OFR 25-84, 1983, 541 pp.

Although the ring yield mechanism worked well in the initial tests, the posts themselves buckled and failed. The joint in the middle of the column added eccentricity to the column, which promoted buckling failure. Several changes were made in the design to produce an acceptable load-yield curve without buckling. The size and shape of the interference ring were specified, and a bevel was added to the leading edge of the interference ring to eliminate the plowing action of the previously sharp edge. (Originally, the 90° angle at the upper edge of the expansion ring would become embedded in the larger pipe and cause gouging of the metal, thus leading to buckling of the post.) Additional testing showed that the bevel and a minimum of 0.5 in of interference between the ID of the larger pipe and the OD of the interference ring resulted in an acceptable load curve and a smooth yielding process (fig. 3).

During the testing, heavy grease was applied to some of the units, and although the general shape of the loading curve did not change, this lowered the load value that could be obtained with a given interference. For example, for a post having an interference of 0.545 in and no grease, a 55-ton load could be achieved before the pipe buckled, but by using the same interference and adding grease, only a 45-ton load could be developed.

Further testing showed that by increasing the interference and greasing the ring, higher loads could be obtained with less likelihood of buckling. In several cases, interferences greater than 0.565 in were used and loads greater than 65 tons were achieved (fig. 4).

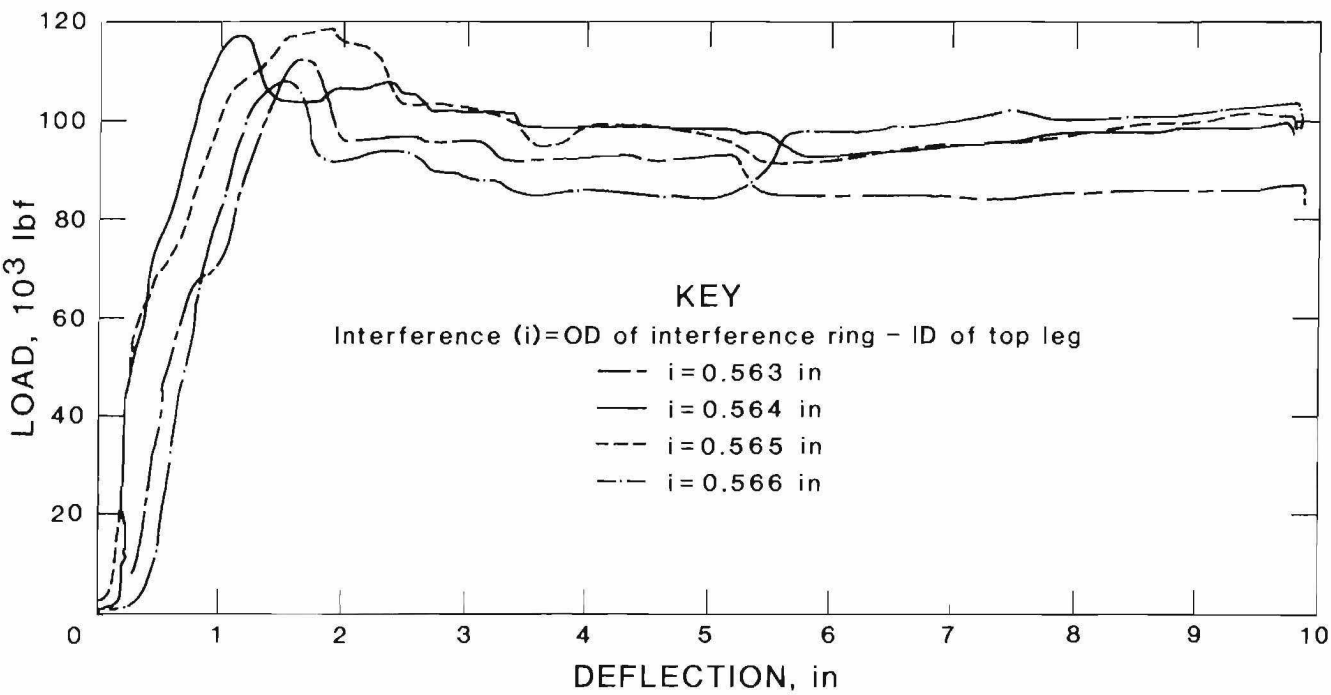

Figure 3.–Load deflection curves for various amounts of ring interference.

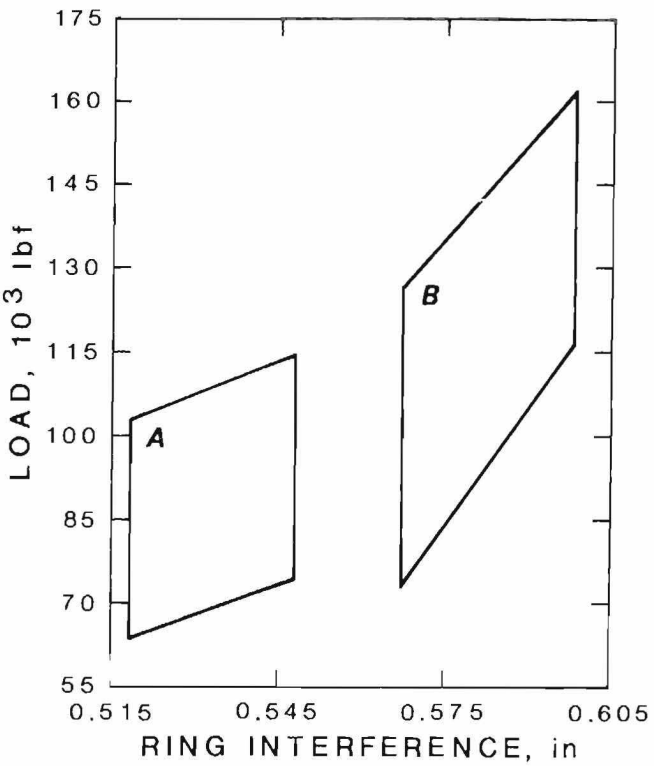

Figure 4.–Compression tests, greased versus ungreased.

In addition, grease reduced the tendency of the post to buckle because there was less gouging of the pipe walls by the expansion ring. Also, when the flared end of the top leg folded back to the bottom leg, the grease prevented the top leg from digging into the bottom leg.

During initial testing of the prototype design, it was found that a large number of variables affected the performance of the post, including the following:

Pipe wall thickness.

The angle of the expansion ring bevel.

The angle of the flaring mandrel.

The actual amount of interference between the expansion ring and the yield leg.

Many of these variables and design problems had been recognized at the outset of research, but as the prototype came closer to meeting original support design specifications, the material and mechanical limits of the post became apparent. This resulted in an increase in the number of laboratory tests required.

It was decided to apply mathematical theory to the post design in an attempt to reduce the number of physical tests needed. The process in which the larger pipe yields is analogous to the metallurgical process of tube expansion (appendix B). In this process, a tube is pushed or pulled over a mandrel to increase tube diameter.

A detailed mathematical analysis of the process of tube expansion has been developed by Avitzur.[4] This analysis is based on elasticity theory and the application of von Mises' yield criterion and the upper-bound theorem. The assumptions required for the Avitzur analysis are that the following three conditions exist:

1. The yielding mechanism acts as a solid, rigid mandrel.
2. A constant friction force is applied during deformation.
3. There is a constant angle of attack between the mandrel and the tube.

Laboratory tests were performed to measure the load required to cause the post to yield. The measured yield forces were lower than those predicted by tube expansion theory. This result can be attributed to the nonrigid action of the expansion ring and the anisotropic behavior at the tube's welded seam. Therefore, the analysis based on expansion theory is more applicable to seamless pipe undergoing concentric loading. Because of the differences between actual results and results obtained from tube expansion theory, additional physical testing was necessary. Therefore, an empirical iterative approach was adopted whereby the results of laboratory testing were used to modify the design in successive steps.

Early testing uncovered the probable causes of differences in the test results. These differences were assigned a test priority based upon their estimated relative importance in causing a difference and the ease with which they could be tested. For example, many tests using schedule 40 bottom legs appeared satisfactory until a larger sample size showed greater-than-expected average load differences for the same interference value. The probable cause was erratic behavior in the expansion ring area because of lack of diametric stiffness. A change to schedule 80 bottom legs increased the weight but provided a more consistent average load performance for a specific interference.

The first test posts had the interference rings positioned near the upper end of the lower leg. By not having a sufficient length of pipe inside the upper leg, there was misalignment where the interference ring and the flared top leg met. By moving the interference ring farther down the bottom pipe, a guide was created.

The position of the expansion ring on the pipe was established as follows. Because the ID varies much more than the OD of pipe, the clearance between the stabilizer-guide at the top of the bottom leg and the inside of the top leg is affected more by the top leg ID than by the bottom leg OD.

The amount of circumferential clearance between the legs and the location of the interference ring on the lower leg are factors that in part determine the degree of parallel alignment between the two legs. The greater the misalignment, the greater the tendency toward buckling. Because

[4]Avitzur, B. Metal Forming Process and Analysis. McGraw-Hill, 1968, 339 pp.

of the variation in clearances in different lots of pipe and also because of differences in the heights of the weld beads inside the top legs, the interference ring was located 16 in from the top after a location of 8 in from the top failed to provide acceptable results. Ideally, the interference ring should be placed at greater than one-half the top leg height, but this was precluded by the desired 70-in minimum height and 24-in convergence range.

To prevent the top of the bottom leg from gouging the inner wall of the top leg when the post was being loaded, the top 0.25 in of the bottom leg was beveled to approximately 8°. If the bottom leg locks because of gouging, the top leg will buckle. The bevel at the top of the bottom leg automatically becomes lubricated as it picks up grease from the inside of the top leg, which then prevents further locking and buckling.

To operate this support, enough clearance was needed to be able to easily fit the two legs together into starting position by hand. Hand-fitting was always possible using ASTM A-120 pipe, but more expensive pipe could not be fitted together by hand without lathing the bottom leg OD smaller than stock. The ID of the lowest priced seamless pipe was more often out-of-round, or oval shaped, than the least expensive ASTM A-120 pipe.

FABRICATION OF YIELDING STEEL POST

The test results led to the development of a functional post design that could be used in highly yielding ground conditions. The post was made from ordinary ASTM A-120 pipe, mild steel plate (for the roof and floor plates), and cylindrical tube stock (for the expansion ring). Materials were purchased precut to standard dimensions. The bottom mounting bracket was constructed by welding the flat plate to a short section of pipe (fig. 1). The roof plate was welded to the top leg in a similar manner.

Easy and consistent entry of the bottom leg into the top leg required a 30° flare on the bottom end of the top leg. A greased mandrel was used to start the flaring at a load of about 12.5 tons and to finish at 30 to 37.5 tons. Flaring stopped when the pipe end reached an OD of 5.125 to 5.25 in. Greater flaring promoted splitting at the open end.

The expansion ring was cut from the cylindrical tube stock to the correct length of 0.5 in. The ring was then welded around the pipe on both the top and bottom of the ring to ensure maximum strength. The top leg ID was then measured. The amount of interference was previously calculated based on the design load of the unit. With the upper leg ID known, the expansion ring was then lathed to the proper OD to produce the correct interference. Grease was then added to the top leg.

FIELD TRIALS

The objective of the field trials was to place the units in a working mine under actual operating conditions. In a mine, the posts could be loaded by a sudden impact, which would be quite a different situation from controlled loading by laboratory equipment

The field test criteria required that the test site have high vertical loads and a large amount of roof-to-floor closure. A Western coal mine with 1,500 to 2,500 ft of overburden in a retreat longwall section met these specifications. At this mine, gate roads are used twice during their lifetime: first as the headgate and then as the tailgate for the adjacent panel. To reduce entry closure, the operator must install double and triple rows of cribs. Even with massive cribbing, there is still a great deal of floor heave between the cribs.

Mine management cooperated with the Bureau by providing advance information concerning the test site and a mine crew to both install the posts and monitor the site visually when Bureau personnel were not present. The mine also obtained the Mine Safety and Health Administration (MSHA) permit required for an experimental support system. The Bureau provided the yielding posts, and Bureau personnel mapped and measured the test site area, coordinated the installation, and retrieved test site data after the posts were installed.

The yielding posts were placed in two test sections. In the first section, 10 posts were installed alongside the wooden crib line. The success of this test and discussions with mine management led to a larger scale second test, where 84 yielding steel posts were placed in two different configurations along 187 ft of headgate entry. Both field tests are described in detail in the following sections.

Trial 1

Ten prototype units were built. The posts were designed to be used in a seam 72 to 84 in high. They had a total potential yield of 23 in, a load capacity of 50 tons, and a weight of 112 lb. In the summer of 1984, these units were installed as supplemental support in the tailgate of the mine over a 90-ft-long entry and 400 ft from the starting point of the longwall. (The mine designation for the longwall panel where the posts were installed is 17th right.)

At the time of installation, the company was having great difficulty maintaining airflow and escapeway clearance through the longwall entries. The 16th right longwall panel had a history of extreme floor heave. In the 16th right panel, the floor heave followed the longwall from 0 to 300 ft behind the face while the entry was used as a headgate. Additional floor heaving occurred while the entries were used as a tailgate. Sometimes this abutment load appeared as much as 50 ft ahead of the longwall face. Total floor heave was often as much as 24 in and pieces of fractured floor would be standing almost vertically in the entry.

As the longwall face proceeded past the test area, all of the posts yielded between 1 and 3 in. Five of the posts had significant yield, indicating that the 50-ton design load had been exceeded. One of these five supports did buckle, leading to the conclusion that the post load capacity should be reduced. After reviewing the laboratory test data, it was felt that a 10% reduction in load capacity (5 tons) would ensure column stability. Furthermore, the 7-in-square top bearing plates proved to be too small. After the longwall passed the area and the ground was highly fractured, the roof fell out around the plate so that eventually the post was only supporting a small column of overlying strata.

Trial 2

After the first field test demonstrated the ability of the post to load quickly and to yield without failing, mine management agreed to a more extensive test of the yielding steel posts. While monitoring the performance of the posts in the first test section, two observations were made that affected post installation in the second test area. First, even though the crib lines were installed close to one another (8-ft centers), the floor would heave between the cribs, causing a reduction in roadway height and in the area of cross section available for ventilation; secondly, track rails used during development of the entries were available for use with the post support system.

After discussing the possible use of the rails during the second field test, the continuous-floor-beam approach was conceived. This approach called for installing yielding steel posts on salvaged track rail. One configuration had two parallel rails down the center of the entry; the posts were mounted every 5 ft on each rail, with an offset of 2.5 ft between the two rails, resulting in a yielding steel post being placed every 2.5 ft (fig. 5). The second configuration had a single rail centered in the entry and a yielding post mounted every 2.5 ft (figs. 5 and 6).

Prior to this test, wooden posts and a center crib line were used with poor results. It was hoped that a continuous-floor-beam yielding support would provide improved support during entry use as both a headgate for the 17th right longwall and subsequently as a tailgate for the 18th right panel. The spacing in the one- and two-rail systems was determined to have the same support characteristics as the wood crib configuration currently being used.

Eighty-six yielding steel posts were fabricated for the second test. Eighty-four were installed and two were reserved for replacement if necessary. With 1,500 ft of cover in the trial site area, loads of 12 tons per linear foot were expected. Twenty-one flat hydraulic stress cells were installed on the posts to measure loads (fig. 7). Based on information from the first trial, the amount of interference between the expansion ring on the inner pipe and the ID of the outer pipe decreased. This lowered the yield load capacity from 50 to 45 tons and thus decreased the possibility of column buckling. A 12-in-square plate was used for a roof plate to increase the load-bearing area. The bottom mounting plate was modified to fit over the track (fig. 8). This included welding flanges on each side for stability.

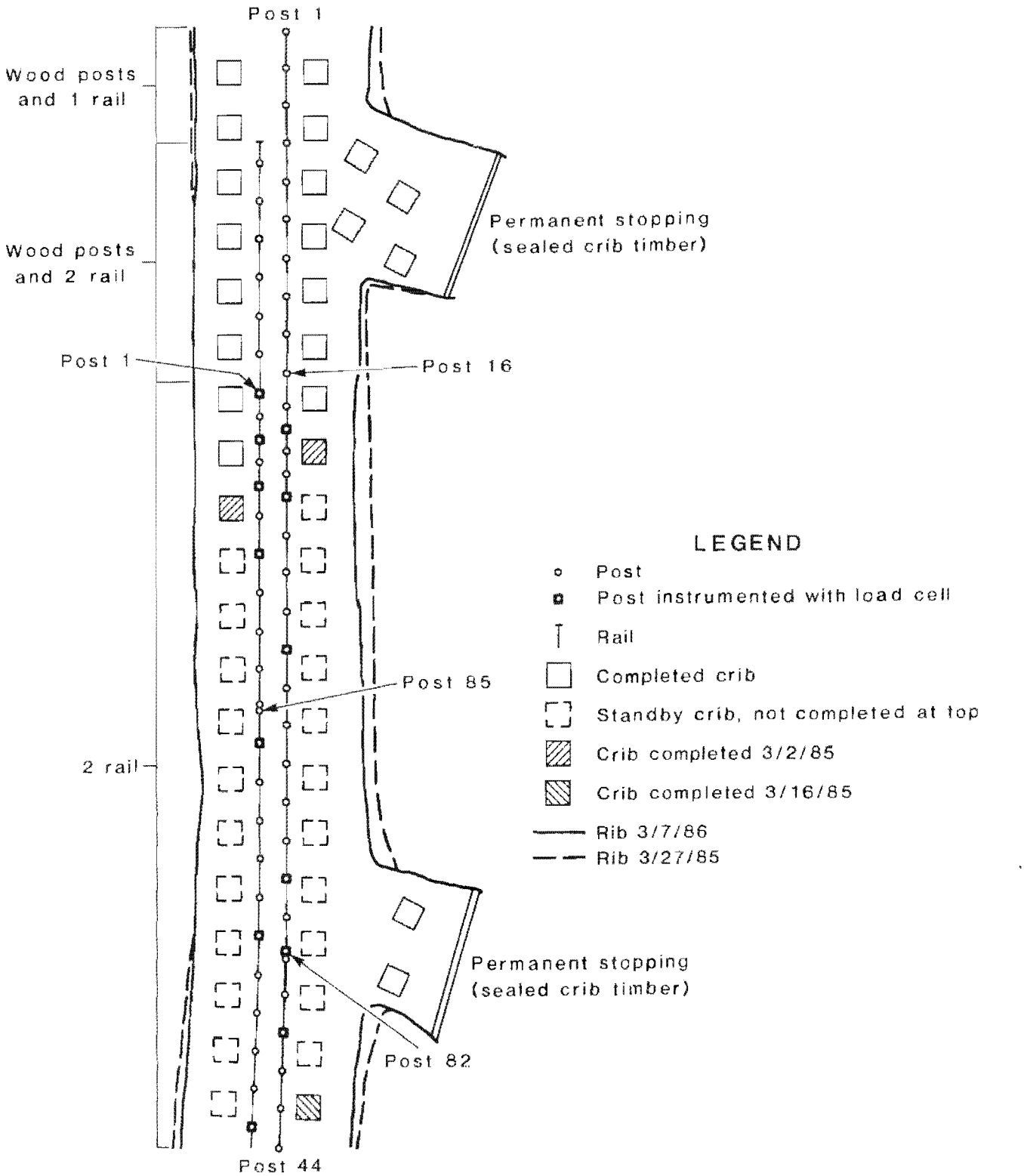

Figure 5.–Test entry, two-rail system.

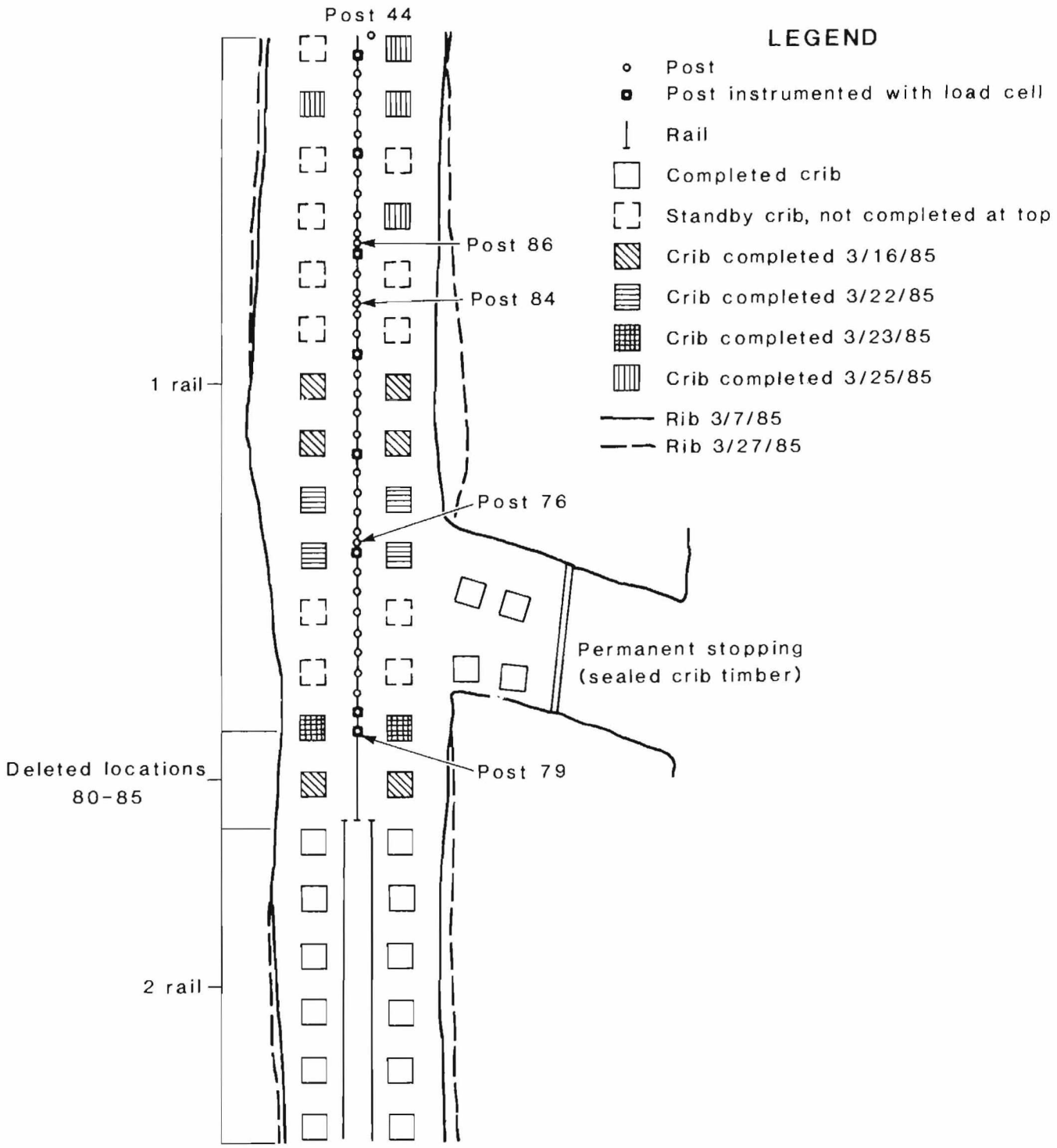

Figure 6.–Test entry, one-rail system.

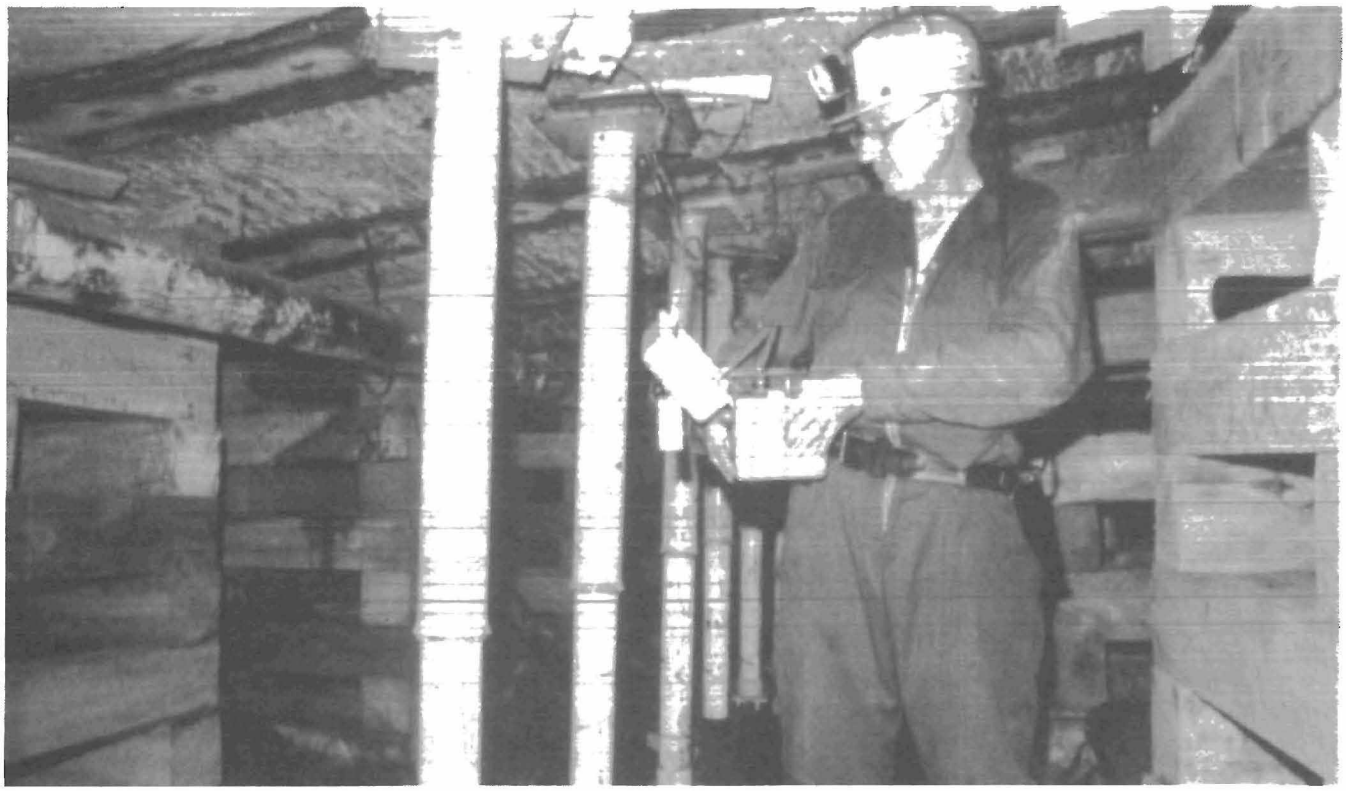

Figure 7.–Monitoring load buildup on yielding steel post.

Figure 8.–Transition from two-rail system to one-rail system.

At the time of this test, a minimum of two and sometimes three rows of cribs with posts had been required to support the entries. Both MSHA and mine management thought it prudent to build the two outside rows of cribs in the test entry, but they did not plan to preload the cribs with wedges until the steel posts and rails showed inadequate support capability. During the first month after installation, loads of 10 tons per linear foot were measured on the posts. After 6 months, the average load on the posts was nearly 12 tons. This 12-ton load agrees with the average load measured by Whittaker[5] under similar conditions in the United Kingdom.

There were some problems in this field test, mainly because of differences in pipe quality. It was noted that some of the manufactured pipe in the 86 test units had slightly thinner walls than pipe purchased earlier. However, wall thickness was still within the specifications for ASTM A-120 seamed pipe. During the flaring operation, some of the pipe split at the weld. Prior to this test, no top legs had split in over 100 flaring operations. Rewelding the split provided enough additional strength to reflare the units. The posts made with the inferior pipe were marked to see how they would perform in the field. After 1 month underground, the splitting problem occurred again (fig. 9).

The mine operator decided to complete installation of the cribs in the test area after 2.5 months. The test site stabilized after the longwall had passed. A followup inspection of the site found that 10 to 20 in of closure were common; however, the section supported with the yielding steel posts was more passable than the section of entry supported with cribs only.

During the summer of 1986, the longwall face passed the second trial site, which was then the tailgate entry. Inspections of the site were made as the longwall retreated to determine how the yielding steel posts responded to the change in conditions.

As was expected from an entry doing double duty as both a headgate and a tailgate, the abutment load ahead of the face and the increasing vertical loads developed by the longwall caused extreme deterioration of the surrounding strata. The posts with the weak welded seams continued to split and the "good" posts yielded still further. There was a noticeable difference in the quality of the test section as compared to areas where only normal crib supports were used. Many of the supports yielded almost to the 24-in maximum.

A necessary point to be considered is the effect of completing the cribs in the test area. Ground conditions in the test entry were broken and heavy, and previous mining had numerous problems dealing with these conditions. At the time the decision was made to complete the cribs, the yielding posts had already started to perform, but the splitting problem justifiably concerned the company. It is still uncertain to what degree either the cribs or the yielding posts contributed to the overall support of the entry. As a minimum, however, it can be said that the condition of the entry was better in the test section than in the areas supported by cribs alone. It remains to be seen if the posts and beams will work by themselves.

[5]Whittaker, P. E. Strata Loading in Mine Roadway Supports. Min. Sci. and Technol., v. 2, No. 1, 1984, pp. 45-46.

Figure 9.–Pipe splitting problem.

CONCLUSIONS

Laboratory and field tests have shown that the yielding steel post is a workable mechanism for supporting ground. Data from the tests support the following conclusions and recommendations:

1. When the posts are used in a floor-beam system adjacent to a crib line, floor heave is reduced in the center of the entry.
2. The two-rail system is better than the one-rail system because it eliminates the need for cribs on the coal rib side of the next longwall panel. However, support is still needed on the chain pillar side.
3. A 45-ton-load capacity is the upper limit for a yielding steel post in the 6- to 7-ft-high range when column buckling, roof punching, and the weight of the unit are considered.
4. Pipe specifications must be rigidly controlled when ordering materials to build the units. Wall thicknesses must be in excess of 0.226 in and ASTM A-120 pipe must be used.

Use of the yielding posts with rails to form floor beams appears to be an acceptable support system. Aside from metallurgical problems with some pipe welds, the support system worked as designed. While the field test showed that the two-rail system was superior to the one-rail system in that it provided more floor-bearing area, additional work needs to be done in determining alternative support patterns, the optimal location of the posts in the entry, and applications in other areas for the support of ground.

APPENDIX A.—CALCULATIONS AND ASSUMPTIONS FOR ECONOMIC COMPARISON

MATERIAL COSTS

This cost comparison contains the following assumptions:

The load capacity for the yielding steel post (YSP) is 40 tons.

The YSP's are spaced on 2-ft centers.

The load capacity for a wood crib is 100-150 tons.

The wood cribs are placed on 6-ft centers.

The weight of a YSP is 120 lb.

The weight of a wood crib is 1,600 lb.

Steel

Cost to fabricate a YSP:

Materials, including welding rod	$ 53.00	
Labor	120.00	
Total	173.00	
Floorbeam, 2 ASCE 60-lb rails at $0.35/lb	14.00	
Cost per foot of entry, $173 ÷ 2 + $14		$100.50

Wood

12 by 12 ft at $450/thousand board feet = $0.45/board foot, crib size equals 40 by 40 by 84 in, therefore cost equals $0.45 × 40 × 14	$252.00	
Cost per foot of entry, $252 ÷ 6 ft		$42.00

INSTALLATION

Steel

Assume that 6 ft of entry is being supported, that the materials are at the work area, and that the posts are set on old track rails.

Because there are fewer pieces to handle with a YSP, the installation will only require a two-person crew, which can install a single post in 15 min. To get the same support capacity as a wood crib, three YSP's will be needed. Therefore, at $30/crew-hour, cost will be $22.50

Wood

Installation of a wood crib that can support the equivalent 120-ton load will require a three-person crew handling 28 crib blocks an hour. Therefore, at $45/crew-hour, cost will be $45.00

APPENDIX B.—EQUATION OF TUBE EXPANSIONS

The method of ground support reported here is analogous to the metallurgical process of tube expansion. In that process, a tube is pulled or pushed over a mandrel to increase the tube diameter. When the tube is pushed over the mandrel, the process is tube extrusion.

A detailed mathematical analysis of the process of tube expansion has been developed by Avitzur.[1] The analysis is based on the results of elasticity theory, the application of von Mises' yield criterion, and the upper-bound theorem. It begins with a consideration of the geometry of material flow through a conical die as shown in figure B-1. A kinematically admissable velocity field is shown in figure B-2. Note that only in zone 2 is material being deformed. In zones 1 and 3, material flows axially. Also note that in zones 1 and 3, the velocity is continuous and remains continuous normal to the surfaces of discontinuity Γ_1 and Γ_2. However, parallel to surfaces Γ_1 and Γ_2, the velocity is discontinuous; that is, to the left of Γ_2 and to the right of Γ_1, the component of velocity parallel to these two surfaces is zero.

The total power of deformation of the material flowing through a conical die is given by

$$J^* = \frac{2}{\sqrt{3}}\sigma_0 \int_V \sqrt{\tfrac{1}{2}\varepsilon_{ij}\varepsilon_{ij}}\, dV + \int_{S_\Gamma} \tau\, \Delta v\, ds - \int_{S_t} T_i v_i\, ds \qquad \text{(B-1)}$$

where σ_0 = tensile yield strength,

ε_{ij} = components of the strain rate tensor,

V = volume of the material,

s_r = surface of velocity discontinuity,

τ = shear stress,

Δv = velocity discontinuity,

s = surface; surface area and surface of stress discontinuity,

s_t = surface over which tractions are prescribed,

T = surface tractions (front or back stresses applied in forming processes),

and v = velocity.[2]

Each term in equation B-1 is expressed in terms of variables relating to the geometry of figure B-2. The result

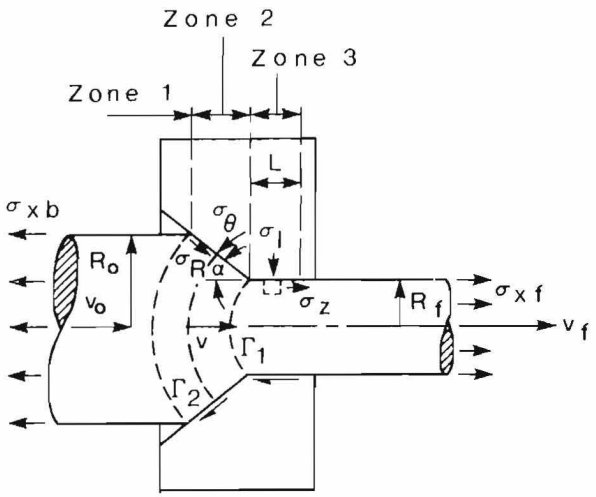

Figure B-1.–Flow of material through conical die. Note that x and z indicate directions of stress.

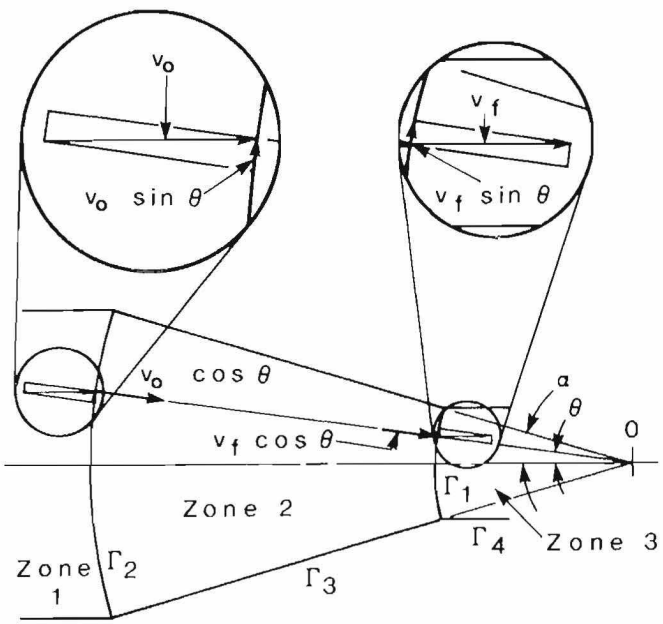

Figure B-2.–Kinematically admissable velocity field.

is set equal to the total externally applied power and is related to the stresses involved.

The first term of equation B-1 is the power of deformation of the total volume of material in zone 2:

$$\dot{W}_i = \int_V w_i dV = \frac{2}{\sqrt{3}}\sigma_0 \int_V \sqrt{\tfrac{1}{2}\varepsilon_{ij}\varepsilon_{ij}}\, dV, \qquad \text{(B-2)}$$

where W_i = power of deformation per unit volume

and w_i = work per unit volume.

[1]Avitzur, B. Metal Forming Process and Analysis. McGraw-Hill, 1968, p. 339.

[2]Prager, W., and P. G. Hodge, Jr. Theory of Perfectly Plastic Solids. Dover, 1968, p. 237.

The second term of equation B-1 takes into account shear power over surfaces of velocity discontinuity and between forming die and material. The last term takes account of stresses applied to the material as it moves through the die. The upper-bound theorem states that "among all kinematically admissable strain-rate fields the actual one minimizes" equations B-1 and B-2. After each term in equation B-1 has been expressed in variables relating to the problem depicted in figure B-1, the resulting expression will be applied specifically to the problem of tube expansion.

Considering the first term of equation B-1, the strain rate components are related to velocity as follows: Set the velocities in spherical coordinates r, θ, and ϕ for convenience as in figure B-3. Then the strain rates in zone 2 are

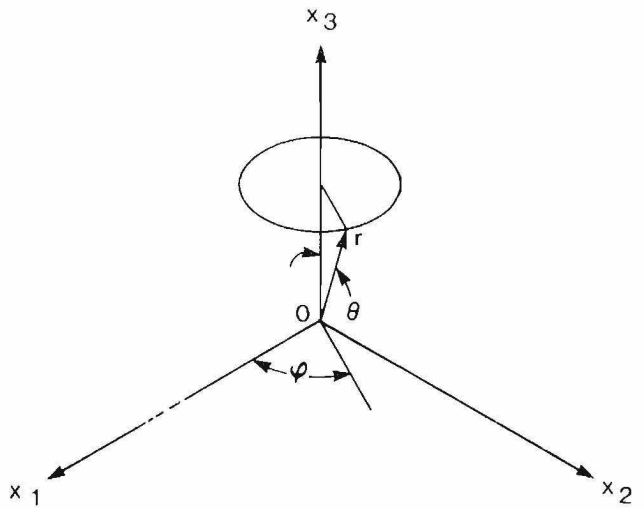

Figure B-3.–Spherical coordinates.

$$\dot{\varepsilon}_{rr} = \frac{d\dot{v}_r}{dr}, \tag{B-3}$$

$$\dot{\varepsilon}_{\theta\theta} = \frac{\dot{v}_r}{r}, \tag{B-4}$$

$$\dot{\varepsilon}_{\phi\phi} = \frac{\dot{v}_r}{r} = -(\dot{\varepsilon}_{rr} + \dot{\varepsilon}_{\theta\theta}), \tag{B-5}$$

$$\dot{\varepsilon}_{r\theta} = \frac{1}{2r}\frac{d\dot{v}_r}{d\theta}, \tag{B-6}$$

and

$$\dot{\varepsilon}_{\theta\phi} = \dot{\varepsilon}_{r\phi} = 0, \tag{B-7}$$

where $\dot{v}_r$ = velocity

and r = position vector.

For material flowing through the conical die of figure B-1, the velocity field is

$$\dot{v}_r = v = v_f r_f^2 \frac{\cos^2\theta}{r^2} \tag{B-8}$$

and

$$\dot{v}_\theta = \dot{v}_\phi = 0. \tag{B-9}$$

The strain rates are then

$$\dot{\varepsilon}_{rr} = 2v_f r_f^2 \frac{\cos\theta}{r^3} = -2\dot{\varepsilon}_{\theta\theta} = -2\dot{\varepsilon}_{\phi\phi}, \tag{B-10}$$

$$\dot{\varepsilon}_{r\theta} = \frac{1}{2} v_f r_f^2 \frac{\sin\theta}{r^3}, \tag{B-11}$$

and

$$\dot{\varepsilon}_{\theta\phi} = \dot{\varepsilon}_{r\phi} = 0. \tag{B-12}$$

Expanding equation B-2 gives

$$\dot{W}_i = \frac{2}{\sqrt{3}}\sigma_0 \int_v \left[\frac{1}{2}(\dot{\varepsilon}_{rr}^2 + \dot{\varepsilon}_{\theta\theta}^2 + \dot{\varepsilon}_{\phi\phi}^2) + \varepsilon_{r\theta}^2 + \varepsilon_{\theta\phi}^2 + \varepsilon_{r\phi}^2\right]^{1/2} dV \tag{B-13}$$

Substituting equations B-10-B-12 into equation B-13 and setting

$$dV = 2\pi\, r \sin\theta\, r\, d\theta\, dr$$

results in

$$\dot{W}_i = 2\sigma_0 v_f r_f^2 \int_{\theta=0}^{\alpha} \left(2\pi\sqrt{1 - \tfrac{11}{12}\sin^2\theta}\,\sin\theta \int_{r=r_f}^{r_0} \frac{dr}{r^3}\right) d\theta$$

$$= 4\pi\sigma_0 v_f r_f^2 \ln\left(\frac{r_0}{r_f}\right) \int_{\theta=0}^{\alpha} \sqrt{1 - \tfrac{11}{12}\sin^2\theta}\,\sin\theta\, d\theta. \tag{B-14}$$

Carrying out the integration with respect to θ equations B-3 through B-7 and rearranging terms give

$$\dot{W}_i = 2\pi\sigma_0 v_f r_f^2 \ln \frac{r_0}{r_f}\left[1 - \cos\alpha\sqrt{1 - \tfrac{11}{12}\sin^2\alpha} + \frac{1 - \frac{11}{12}}{\sqrt{\frac{11}{12}}} \ln \frac{\sqrt{\frac{11}{12}} + 1}{\sqrt{\frac{11}{12}}\cos\alpha + \sqrt{1 - \frac{11}{12}\sin^2\alpha}}\right]. \tag{B-15}$$

From constancy of volume

$$\frac{r_0}{r_f} = \frac{R_0}{R_f} \tag{B-16}$$

where R = radius.

Also

$$r_f = R_f/\sin\alpha. \tag{B-17}$$

Substituting equations B-16 and B-17 into equation B-15 yields for the first term of equation B-1

$$\dot{W}_i = 2\pi\sigma_0 v_t R_f^2 f(\alpha) \ln \frac{R_0}{R_f} \tag{B-18}$$

where

$$f(\alpha) = \frac{1}{\sin^2\alpha}\left[1 - (\cos\alpha)\sqrt{1 - \tfrac{11}{12}\sin^2\alpha} + \frac{1}{\sqrt{11 \cdot 12}} \times \ln \frac{1 + \sqrt{\frac{11}{12}}}{\sqrt{\frac{11}{12}}\cos\alpha + \sqrt{1 - \frac{11}{12}\sin^2\alpha}}\right]. \tag{B-19}$$

The second term of equation B-1 is formulated by first making use of the von Mises' yield criterion, the result of which is that the shear stress component in zone 2 cannot exceed the value $\tau = \sigma_0/\sqrt{3}$. On this basis, the second term of equation B-1 for the surfaces Γ_1 and Γ_2 is

$$\dot{W}_{s_{1,2}} = \int_{\Gamma_1,\Gamma_2} \tau\,\Delta v\,ds = \int_{\Gamma_1} \tau\Delta v\,dA + \int_{\Gamma_2} \tau\,\Delta v\,dA\,. \tag{B-20}$$

The velocity discontinuity is

$$\Delta v = v_f \sin\theta \tag{B-21}$$

and the area is

$$dA = 2\pi r f \sin\theta\, r_f\, d\theta. \tag{B-22}$$

Equation B-20 is then

$$\dot{W}_{s_{1,2}} = 4\pi v_f r_f^2 \frac{\sigma_o}{\sqrt{3}} \int_{\theta = 0}^{\alpha} \sin^2\theta\, d\theta. \tag{B-23}$$

Integrating and substituting for r_f from equation B-17 give

$$\dot{W}_{s_{1,2}} = \frac{2}{\sqrt{3}} \sigma_0 \pi \upsilon_t R_f^2 \left(\frac{\alpha}{\sin^2 \alpha} - \cot \alpha \right). \tag{B-24}$$

The frictional power losses along the surface between the die and the material Γ_3 are obtained as follows: The velocity discontinuity is

$$\Delta \upsilon = \upsilon_t r_f^2 \frac{\cos \alpha}{r^2} \tag{B-25}$$

and an element of area of surface Γ_3 is

$$ds = 2\pi R \frac{dR}{\sin \alpha}. \tag{B-26}$$

Assuming constant shear friction,

$$\tau = m \frac{\sigma_0}{\sqrt{3}} \quad , 0 \quad \dot{m} \quad 1. \tag{B-27}$$

The power of deformation due to frictional losses along Γ_3 is from equation B-28

$$\dot{W}_{s_3} = \int_{\Gamma_3} \tau \, \Delta \upsilon \, ds = \int_{R = R_f}^{R_0} \frac{2\pi R}{\sin \alpha} \upsilon_t \left(\frac{R_f}{R} \right)^2 (\cos \alpha) m \frac{\sigma_0}{\sqrt{3}} dR \tag{B-28}$$

$$= \frac{2}{\sqrt{3}} \sigma_0 m \pi \upsilon_t R_f^2 (\cot \alpha) \ln \frac{R_0}{R_f}. \tag{B-28}$$

The sum of equations B-24 and B-28 gives the total power of deformation along surfaces of discontinuity.

The third term of equation B-1 will be formulated after introduction of the geometry of tube expansion.

Finally, the total power of deformation is set equal to the externally applied power which contains the applied traction stress,

$$J^* = \pi \upsilon_f (R_{of}^2 - R_{if}^2) \sigma_{xf} = \pi \upsilon_f R_{if}^2 \left[\left(\frac{R_o}{R_i} \right)^2 - 1 \right] \sigma_{xf}. \tag{B-29}$$

The geometry of tube expansion is shown in figure B-4. A tube of inside radius R_i is forced over the mandrel to increase the inside radius to R_{if}. From the geometry of figure B-4

$$\frac{\sin \alpha}{R_i} = \frac{\sin \alpha_0}{R_f} \tag{B-30}$$

and

$$\frac{R_{of}}{R_o} = \frac{R_{if}}{R_i} \tag{B-31}$$

where R_o = outside radius.

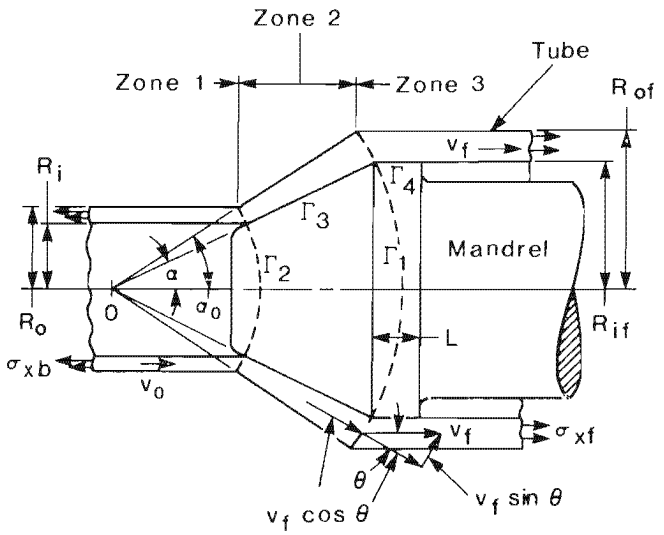

Figure B-4–Geometry of tube expansion.

Applying equation B-18 to tube expansion gives for the internal power of deformation

$$\dot{W}_i = 2\pi\sigma_0 v_t \left[R_{of}^2 f(\alpha_0) \ln\frac{R_o}{R_{of}} - R_{if}^2 f(\alpha) \ln\frac{R_i}{R_{if}}\right] = 2\pi\sigma_0 v_t \frac{R_{if}^2}{\sin^2\alpha}\left[f(\alpha_0)\sin^2\alpha_0 - f(\alpha)\sin^2\alpha\right] \ln\frac{R_{if}}{R_i}. \quad \text{(B-32)}$$

Applying equation B-24 to tube expansion yields the power along surfaces of velocity discontinuity Γ_1 and Γ_2

$$\dot{W}_{s_{1,2}} = \frac{2}{\sqrt{3}}\sigma_0\pi v_f R_{if}^2\left[\frac{R_o}{R_i}\right]^2\left[\left[\frac{\alpha}{\sin^2\alpha_o} - \cot\alpha_0\right] - \left[\frac{R_i}{R_o}\right]^2 \left[\frac{\alpha}{\sin^2\alpha} - \cot\alpha\right]\right]. \quad \text{(B-33)}$$

Applying equation B-28 to the surface Γ_3 gives frictional loss

$$\dot{W}_{s_3} = \frac{2}{\sqrt{3}}\sigma_0 m\pi v_t R_{if}^2 (\cot\alpha) \ln\frac{R_{if}}{R_i}. \quad \text{(B-34)}$$

Frictional losses along the length, L, of contact between mandrel and tube are included as

$$\dot{W}_{s_4} = \frac{2}{\sqrt{3}}\sigma_0 m\pi v_t R_{if} L. \quad \text{(B-35)}$$

The third term of equation B-1 applied to tube expansion is

$$\dot{W}_b = -\int_{s_t} T v_i \, ds = \pi v_0 (R_o^2 - R_i^2)\sigma_{xb} = \pi v_t (R_{of}^2 - R_{if}^2)\sigma_{xb} = \pi v_t R_{if}^2\left[\left(\frac{R_o}{R_i}\right)^L - 1\right]\sigma_{xb}. \quad \text{(B-36)}$$

Summing equations B-32 through B-34 gives the total power of deformation J* and setting the result equal to equation B-29 gives

$$2\pi\sigma_0 v_t \frac{R_{if}^2}{\sin^2\alpha}\left[f(\alpha_0)\sin^2\alpha_0 - f(\alpha)\sin^2\alpha\right]\ln\frac{R_{if}}{R_i} = \frac{2}{\sqrt{3}}\sigma_0\pi v_t R_{if}^2$$

$$\times\left\{\left(\frac{R_o}{R_i}\right)^2\left(\frac{\alpha_0}{\sin^2\alpha_0} - \cot\alpha_0\right) - \left(\frac{\alpha}{\sin^2\alpha} - \cot\alpha\right) + m\left[\cot\alpha\ln\left(\frac{R_{if}}{R_i}\right) + \frac{L}{R_{if}}\right]\right\}$$

$$+ \pi v_t R_{if}^2\left[\left(\frac{R_o}{R_i}\right)^2 - 1\right]\sigma_{xb} = \pi v_t R_{if}^2\left[\left(\frac{R_o}{R_i}\right)^2 - 1\right]\sigma_{xf}. \qquad \text{(B-37)}$$

Rearranging gives

$$\frac{\sigma_{xf}}{(2/\sqrt{3})\sigma_0} = \frac{\sigma_{xb}}{(2/\sqrt{3})\sigma_o} + A \qquad \text{(B-38)}$$

where

$$A = \frac{1}{(R_o/R_i)^2 - 1}\left\{\sqrt{3}\,F(\gamma)\ln\left(\frac{R_{if}}{R_i}\right) - \left(\frac{\alpha}{\sin^2\alpha} - \cot\alpha\right)\right.$$

$$\left. + m\left[\cot\alpha\ln\left(\frac{R_{if}}{R_i}\right) + \frac{L}{R_{if}}\right] + \left(\frac{R_o}{R_i}\right)^2\left(\frac{\alpha_0}{\sin^2\alpha_0} - \cot\alpha_0\right)\right\} \qquad \text{(B-39)}$$

and

$$F(\gamma) = \frac{1}{\sin^2\alpha}\left\{\cos\alpha\sqrt{1 - \tfrac{11}{12}\sin^2\alpha} - \cos\alpha_0\sqrt{1 - \tfrac{11}{12}\sin\alpha_0} + \frac{1}{\sqrt{11\cdot 12}}\ln\frac{\sqrt{\tfrac{11}{12}}\cos\alpha + \sqrt{1 - \tfrac{11}{12}\sin^2\alpha}}{\sqrt{\tfrac{11}{12}}\cos\alpha_0 + \sqrt{1 - \tfrac{11}{12}\sin^2\alpha_0}}\right\} \qquad \text{(B-40)}$$

Equation B-38 estimates the stress σ_{xb} required to extrude the smaller diameter tube over the mandrel. Where no other stress is applied to the work, α_{xf} is zero. The force required for extrusion is then

$$F = -\pi(R_o^2 - R_i^2)\sigma_{xb}. \qquad \text{(B-41)}$$

Equation B-38 also contains dimensional constants, angles, and friction factor. When $\alpha < \alpha_0 < 65°$, $f(\alpha) \approx f(\alpha_0) \approx 1$ within 5% and the constant A can be approximated by

$$A = \sqrt{3}\ln\frac{R_{if}}{R_i} - \frac{1}{\left(\frac{R_o}{R_i}\right)^2 - 1}\left\{\left(\frac{\alpha}{\sin^2\alpha} - \cot\alpha\right) - m\left[\cot\alpha\ln\frac{R_{if}}{R_i} + \frac{L}{R_{if}}\right] - \left(\frac{R_o}{R_i}\right)^L\left(\frac{\alpha_0}{\sin^2\alpha_0} - \cot\alpha_0\right)\right\} \qquad \text{(B-42)}$$